

## Binding of the Pepper Alkaloid Piperine to Bovine $\beta$ -Lactoglobulin: Circular Dichroism Spectroscopy and Molecular Modeling Study

FERENC ZSILA,<sup>\*,†</sup> ESZTER HAZAI,<sup>†</sup> AND LINDSAY SAWYER<sup>§</sup>

Department of Molecular Pharmacology, Institute of Biomolecular Chemistry, Chemical Research Center, Budapest, P.O. Box 17, H-1525, Hungary, and Institute of Structural and Molecular Biology, School of Biological Sciences, Swann Building, King's Buildings, The University of Edinburgh, Mayfield Road, Edinburgh EH9 3JR, Scotland

The pepper alkaloid piperine is a nontoxic, natural dietary compound with a broad range of physiological activity. The present work is the first demonstration of its interaction with a mammalian protein. Circular dichroism (CD) spectroscopy was used to reveal and analyze the binding of piperine to a lipocalin protein. Induced CD spectra measured in pH 7.7 phosphate buffer at 37 °C demonstrated reversible, non-covalent association of piperine with bovine  $\beta$ -lactoglobulin (BLG), the major whey protein in milk. The binding parameters ( $K_a \approx 8 \times 10^4 \text{ M}^{-1}$ ,  $n = 0.8$ ) determined from the CD titration data showed no significant differences between the piperine binding properties of the two main genetic variants of BLG (A and B). The vanishing extrinsic CD signal obtained upon acidification of the piperine–BLG sample solution (Tanford transition) suggested that the ligand binds in the central hydrophobic cavity of the  $\beta$ -barrel. The cavity binding concept was further supported by a CD displacement experiment using palmitic acid, the well-known hydrophobic ligand of BLG. Molecular docking calculations showed that piperine can be efficiently accommodated within the calyx of BLG. Additional molecular modeling calculations indicated that the  $\beta$ -barrel of human tear lipocalin, human serum retinol binding protein, and human neutrophil gelatinase associated lipocalin might also accommodate a piperine molecule.

**KEYWORDS:** Piperine; bovine  $\beta$ -lactoglobulin; circular dichroism spectroscopy; induced chirality; lipocalin

### INTRODUCTION

Piperine (**Figure 1**) is the main active principle of the widely consumed dietary spice black pepper (*Piper nigrum*) and long pepper (*Piper longum*), which have been used in traditional medicine from ancient times. Piperine shows beneficial biological effects such as protection against oxidative stress (1, 2), inhibition of P450 isoenzymes and monoamine oxidases (3, 4), and antitumor (5, 6), immunomodulatory (5, 7), and antiprotzoic activities (8). At a molecular level, however, its mechanism of action is poorly understood, and no binding interaction of piperine with any biopolymers has been reported in the literature so far.

The lipocalin superfamily consists of functionally diverse proteins that generally bind small, hydrophobic ligands and interact with cell-surface receptors (9, 10). The family is defined by a highly conserved fold; the core structure consists of an eight-stranded antiparallel  $\beta$ -barrel that defines a calyx, or cup-shaped, ligand binding site. Bovine  $\beta$ -lactoglobulin (BLG),

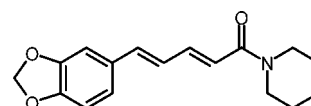


**Figure 1.** Chemical structure of piperine.

abundant in cow's milk, is a typical lipocalin protein (11, 12). The X-ray structure of BLG has been determined and its ligand binding site characterized in detail; it was shown to bind biochemically important agents such as cholesterol, vitamin D (12), fatty acids (13, 14), and retinoids (15). As has been proposed earlier, the inexpensive, commercially available BLG, or its protein-engineered forms, could be used as a versatile carrier of hydrophobic molecules in controlled delivery applications (16, 17). Accordingly, searching for, and finding, novel bioactive ligand molecules of BLG is of biotechnological/pharmacological importance and could contribute to the deeper understanding of the molecular recognition properties of this lipocalin.

By using circular dichroism (CD) spectroscopy, the present work demonstrates the binding of piperine to BLG. The induced CD curves of piperine measured in the presence of BLG are the first experimental evidence for the binding interaction of

\* Corresponding author [fax (+36) 1-325-7750; e-mail zsferi@chemres.hu].

<sup>†</sup> Institute of Biomolecular Chemistry.

<sup>§</sup> The University of Edinburgh.

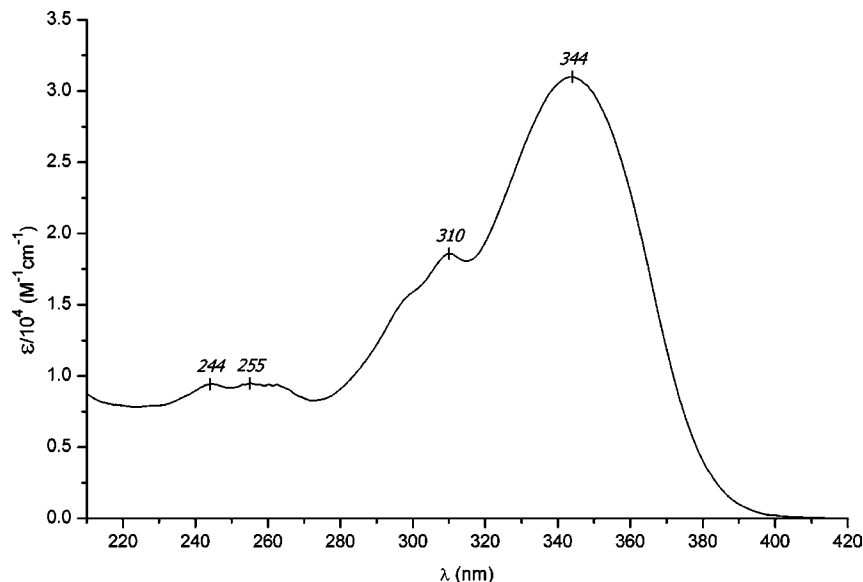


Figure 2. UV absorption spectrum of piperine in ethanol ( $4.4 \times 10^{-5}$  M, cell length = 1 cm, 20 °C).

this alkaloid with a mammalian protein and suggest that piperine may bind to other lipocalins as well. The latter assumption was tested by computational docking calculations performed using the X-ray structures of some human lipocalin proteins.

## MATERIALS AND METHODS

**Materials.** BLG genetic variants A and B and the mixture of A and B (three times crystallized) were obtained from Sigma and used as supplied. Piperine (98%) was purchased from ABCR Group (Karlsruhe, Germany); double-distilled water and HPLC grade organic solvents were used. All other chemicals were of analytical grade.

**Preparation of Protein Sample Solution.** The concentration of the BLG sample solutions made up in 0.01 M (pH 7.7) phosphate buffer was determined spectrophotometrically by using  $\epsilon_{278 \text{ nm}} = 17600 \text{ M}^{-1} \text{ cm}^{-1}$  (16). The molecular weight of BLG was taken to be 18300.

**Preparation of Piperine Stock Solution.** The concentration of the ethanolic solution of piperine was calculated by measuring the optical density at 344 nm;  $\epsilon_{344 \text{ nm}} (\text{EtOH}) = 31000 \text{ M}^{-1} \text{ cm}^{-1}$  (18).

**CD and UV Absorption Spectroscopy.** CD and UV spectra were recorded between 295 and 420 nm on a Jasco J-715 spectropolarimeter at 37 and  $20 \pm 0.2$  °C under a nitrogen flow. Temperature control was provided by a Peltier thermostat equipped with magnetic stirring for the cuvette. A cuvette of 1 cm path length (Hellma USA, Plainview, NY) was used. Each spectrum was signal-averaged at least three times with a bandwidth of 1.0 nm and a resolution of 0.5 nm at a scan speed of 100 nm/min. The UV spectra were obtained by conversion of the high-voltage (HT) values of the photomultiplier tube of the CD equipment into absorbance. CD spectra were recorded and displayed as  $\Theta$  (ellipticity) in units of millidegrees (mdeg). Induced CD spectra resulting from the interaction of the piperine with BLG were obtained by subtracting the CD spectrum of the protein from that of the complex. The quantity  $\Theta$  is converted to  $\Delta\epsilon$  values (see Figure 3) using the equation  $\Delta\epsilon = \Theta/(33982cl)$ , where  $\Delta\epsilon$  is the molar circular dichroic absorption coefficient expressed in  $\text{M}^{-1} \text{ cm}^{-1}$ ,  $c$  is the concentration of the sample expressed in mol/L, and  $l$  is the path length through the cell expressed in cm.

During the CD spectroscopic titrations of BLG with piperine, ethanol content (added with the ligand) never exceeded 2% (v/v). By applying Fourier transform infrared spectroscopy, Dufour et al. (19) have shown that the secondary structure of BLG is unaffected by EtOH at concentrations up to ~20% (v/v), so we are confident that the 10-fold lower concentration will have no effect upon the protein structure.

**Calculation of the Association Constant of Piperine–BLG Complexes.** The stereospecific interaction between a ligand (L) and

its primary site on the protein (P) may be quantified by the association constant ( $K_a$ ):

$$L + P \rightleftharpoons LP; K_a = \frac{[LP]}{[L][P]} \quad (1)$$

It is evident that

$$[L] = c_L - [LP] \quad (2)$$

and

$$[P] = c_P - [LP] \quad (3)$$

where  $c_L$  and  $c_P$  represent the total concentrations of the ligand and protein, respectively.

Because the formation of ligand–protein complexes is responsible for the induced CD activity, it can be written that

$$\Theta \text{ (mdeg)} = k[LP] \quad (4)$$

where  $k$  is a constant.

Using eqs 1–4, we obtain

$$\Theta \text{ (mdeg)} = \frac{k}{2} [c_P + c_L + K_a^{-1} - \sqrt{(c_P + c_L + K_a^{-1})^2 - 4c_P c_L}] \quad (5)$$

To calculate the optimal value of  $K_a$ , nonlinear regression analysis of the CD titration data was performed (NLREG statistical analysis program, v. 6.3, created by Philip H. Sherrod).

**Molecular Modeling Calculations of Piperine–Lipocalin Interactions.** Geometry optimization of piperine was carried out with the Sybyl 6.6 program (Tripos Inc., St. Louis, MO) using the MMFF94 force field and applying the Powell conjugate gradient method. The Autodock 3.0 program package was used for mapping the energetically most favorable binding of piperine to native BLG-A and three human lipocalins. The three-dimensional coordinates of the X-ray structures of BLG-A, human tear lipocalin (TL), human neutrophil gelatinase associated lipocalin (NGAL), and human serum retinol binding protein (RBP) were obtained from the Protein Data Bank (PDB entries 1QG5, 1XKI, 1DFV, and 1JYD, respectively). Gasteiger–Huckel partial charges were applied both for the ligand and for the proteins. Solvation parameters were added to the protein coordinate files, and the ligand torsions were defined using the Addsol and Autotors utilities, respectively. The atomic affinity grids were prepared with 0.375 Å spacing by the Autogrid program for the whole protein target. Random starting

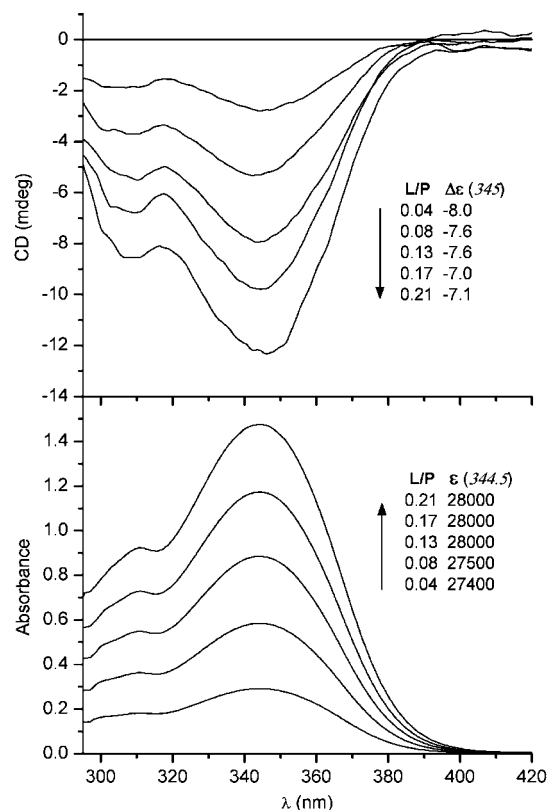


**Figure 3.** Some representative induced CD curves and UV spectra of piperine–BLG (a mixture of genetic variants A and B) complex prepared in 0.01 M (pH 7.7) phosphate buffer solution (cell length = 1 cm; [BLG] =  $2.5 \times 10^{-4}$  M, 37 °C). Ligand/protein molar ratios (L/P), molar absorption ( $\epsilon$ ), and circular dichroic absorption coefficients ( $\Delta\epsilon$ ) are shown.

positions, orientations, and torsions (for flexible bonds) were used for the ligand; each docking run consisted of 100 cycles.

## RESULTS AND DISCUSSION

### UV Absorption Spectrum of Piperine in Organic Solution.

The UV spectrum of piperine recorded in ethanol shows three main regions of absorption (**Figure 2**): the strongest band is present at 344 nm ( $\epsilon = 31000 \text{ M}^{-1} \text{ cm}^{-1}$ ), followed by a less intense, partially resolved peak showing vibrational fine structure around 300 nm ( $\epsilon_{310\text{nm}} = 18600$ ), whereas between 230 and 270 nm a third, low-intensity absorption can be observed with  $\epsilon \sim 1000$ . The molecule can be considered as an aggregate of two different groups that are electronically conjugated: a methylenedioxybenzene and an oxopentadienyl chromophore. Accordingly, these chromophoric parts do not act independently, rather they form a common conjugated  $\pi$ -system in which  $\pi$ - $\pi^*$  transition is responsible for the longest wavelength intense, but structureless, UV band. The intensity of this band indicates that the  $\pi$ - $\pi^*$  transition is electronic dipole allowed; the transition dipole moment lies in the plane of the molecule and is oriented about the long axis of piperine. The second band at 310 nm can be assigned to the  $^1L_b$  transition of the phenyl moiety, which is a symmetry forbidden, weak band in the spectrum of unsubstituted benzene ( $\epsilon \approx 500\text{--}600 \text{ M}^{-1} \text{ cm}^{-1}$ ). Because the wave function symmetry of the aromatic ring is strongly perturbed by the conjugative effect of the double bonds and by the nonbonding electrons of the methoxy groups, the intensity of the  $^1L_b$  band greatly increases and its maximum is shifted to longer wavelengths.

**Binding of Piperine to Bovine  $\beta$ -Lactoglobulin.** Because piperine has no element of chirality, it does not show CD activity

in either organic or aqueous solutions (data not shown). However, when piperine was added to a buffered solution of BLG (a mixture of genetic variants A and B), CD bands appeared in the near-UV and UV spectral regions, respectively (**Figure 3**). These negative Cotton effects (CE) are induced by the asymmetric environment of BLG to which piperine is bound. The shape and spectral position of the CEs are highly similar to those of the absorption peaks, and the CD/UV curves are practically in mirror image relation. The extrinsic CD activity of piperine is moderate; the maximum value of the molar dichroic absorption coefficient ( $\Delta\epsilon$ ) is  $\approx -8 \text{ M}^{-1} \text{ cm}^{-1}$  (**Figure 3**). Absorption spectral characteristics of the UV peaks of the protein-bound piperine, the shape, width, and wavelength of maxima/minima of which were very similar to the curve measured in EtOH, suggest no significant conformational alteration (i.e., twist) of the conjugated  $\pi$  system. Thus, the generation of a particular helical conformation of piperine at the binding site as the source of the observed extrinsic CD bands is unlikely. Furthermore, binding of two piperine molecules to BLG in close vicinity to each other would result in a positive–negative CD band pair due to the chiral intermolecular exciton coupling between their  $\pi$ - $\pi^*$  excited states (20). Additionally, simultaneous binding of two (or more) piperine molecules at different and distantly separated binding sites would induce distinct types of CD band patterns. In such a case, in parallel with increasing ligand concentration, the shape and wavelength positions of the induced CD bands should be changed due to the varying ratio of the bound piperine molecules at the different binding sites having different CD activities. However, CD and UV spectral features of the BLG-bound piperine were unaltered when its concentration was increased in the sample solution (**Figure 3**). As a source of the measured induced CD spectra, however, another mechanism should also be considered, namely, the nondegenerate exciton coupling (21) between the  $\pi$ - $\pi^*$  transitions of piperine and adjacent aromatic residues of the binding site, especially tryptophan, which has an intense absorption band ( $\epsilon \approx 35000 \text{ M}^{-1} \text{ cm}^{-1}$ ) around 220 nm sufficient for excited-state dipole–dipole interaction with ligand chromophores. Of the two Trp residues of BLG, Trp61 is positioned superficially in the flexible loop region on the edge of the entrance of the central pocket while Trp19 is located deep in the calyx as the part of a hydrophobic cluster. Thus, in the case of cavity binding of a given ligand, coupled-oscillator interaction of the Trp19 transition with that of the ligand chromophore can reasonably be expected. Notably, this mechanism was proposed by Fugate and Song (22) for the induced optical activity of BLG–retinol complexes, who reported the maximum  $\Delta\epsilon$  value to be  $\sim -8 \text{ M}^{-1} \text{ cm}^{-1}$  (343 nm) for the extrinsic CD band of retinol (cf. **Figure 3**).

In summary, these results indicate that piperine molecules uniformly bind to the same region of the protein as retinol and that they bind as monomers without significant conformational alteration.

The series of induced CD spectra obtained by repeated additions of piperine to a buffered BLG solution (a mixture of genetic variants A and B) was used to determine the association constant ( $K_a$ ) and the number of binding sites ( $n$ ). Nonlinear regression analysis was performed by fitting a curve to the induced CD data points (**Figure 4**). Using the equation given under Materials and Methods, a good fit was achieved, resulting in values of  $8.28 \times 10^4 \text{ M}^{-1}$  for the association constant ( $K_a$ ) and 0.93 for  $n$ , indicating a single piperine binding site per protein monomer. Because cow's milk commonly contains two genetic forms of BLG called variants A and B, differing at

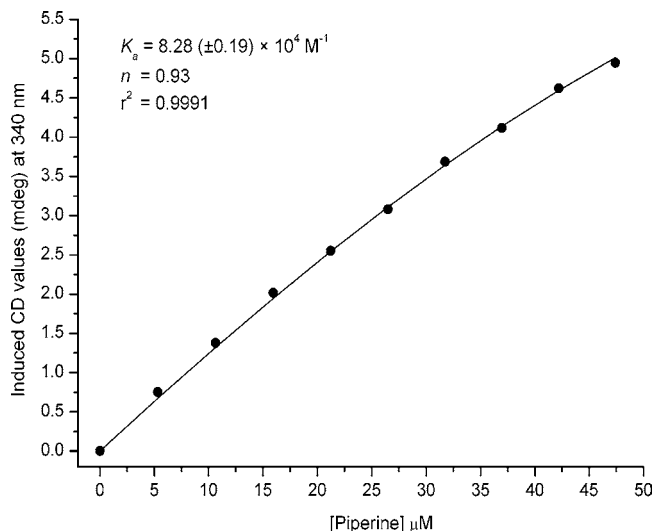


**Figure 4.** Nonlinear regression analysis of piperine–BLG (a mixture of genetic variants A and B) interaction by using CD titration data performed with NLREG software (v. 6.3). Values of the association constant ( $K_a$ ), number of binding sites ( $n$ ), and correlation coefficient ( $r^2$ ) are shown [[BLG] =  $6.3 \times 10^{-5}$  M, 0.01 M (pH 7.7) phosphate buffer, 37 °C].

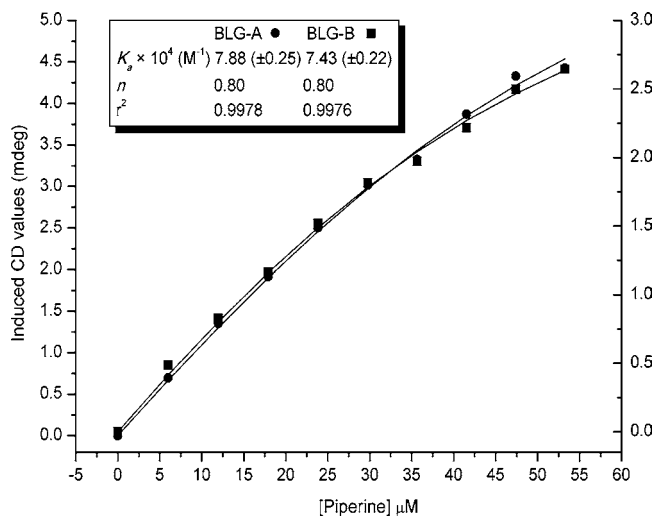


**Figure 5.** Nonlinear regression analysis of the CD titration data obtained by genetic variants A (left axis) and B (right axis) of BLG. Induced CD values (multiplied by  $-1$ ) obtained at 342 and 340 nm were evaluated with NLREG software (v. 6.3). Derived values of the association constants ( $K_a$ ), number of binding sites ( $n$ ), and correlation coefficients ( $r^2$ ) are shown [[BLG-A] =  $6.3 \times 10^{-5}$  M, [BLG-B] =  $5.4 \times 10^{-5}$  M, 0.01 M (pH 7.7) phosphate buffer, 37 °C].

two amino acids (Asp64 is substituted for Gly and Val118 for Ala in variant B), additional CD titration measurements were taken using the pure forms of the two variants to compare their piperine binding properties. According to **Figure 5**, the binding parameters obtained with the A and B variants are very similar, indicating that the residues mentioned above do not play significant roles in piperine binding to the protein.

As shown by the X-ray structures of BLG complexed with fatty acids and retinoids (13–15), the principal binding site of these hydrophobic ligands is the central pocket of the protein; thus, it can be anticipated that piperine also binds here. The distinct pH-dependent conformational change of BLG can be exploited to test such an assumption, to confirm or reject the central cavity binding of a given ligand. There are four flexible loops at the open end of the main binding pocket, referred to

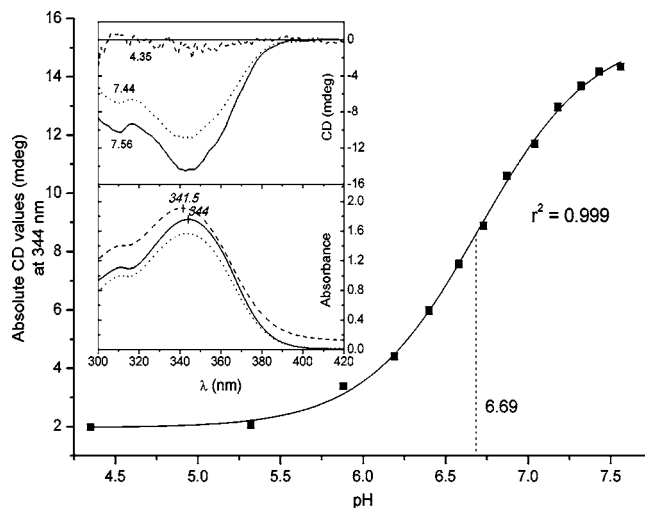


**Figure 6.** CD–pH titration of the piperine–BLG (A + B) solution; 0.01 M phosphate buffer, 37 °C, [BLG] =  $2.5 \times 10^{-4}$  M, [piperine] =  $6.3 \times 10^{-5}$  M. The line represents the curve fit obtained with the program Microcal Origin. (Inset) CD and UV spectra of the starting (pH 7.56) and of the most acidic solutions (pH 4.35) with the spectra obtained by setting the pH value back from 4.35 to 7.44.

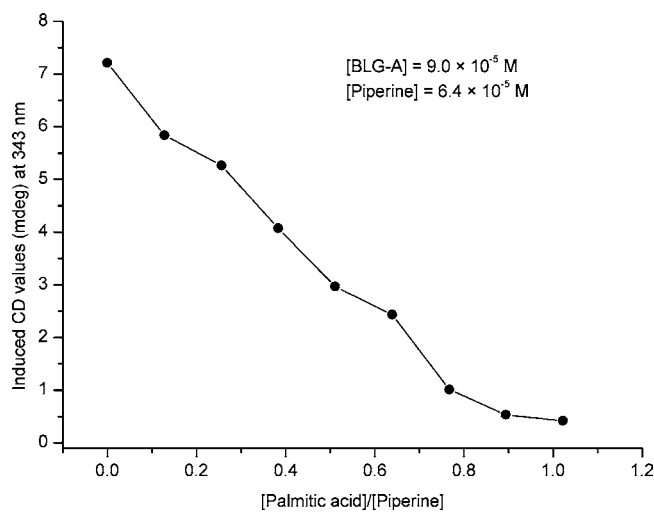


**Figure 7.** CD titration of the piperine–BLG-A complex with palmitic acid in 0.01 M (pH 7.4) phosphate buffer solution at 37 °C.

as the AB, CD, GH, and EF loops, respectively, of which the EF loop (residues 85–90, see **Figure 8**) gates access to the binding site in the central calyx. Reversible conformational movement of this loop occurs between pH 6.5 and 8.0 (23); it serves as a lid that blocks access to the interior of the calyx below pH 6.5. Triggered by the protonation of Glu89 in the EF loop, it flips away at neutral and alkaline pH values and the cavity becomes accessible for the ligand molecule (24). Accordingly, if the piperine is bound in the cavity, the induced CD spectra should be pH dependent; due to the unfavorable steric interactions arising from the piperine molecule and the EF loop residues, the complex should dissociate at acidic pH, resulting in the vanishing of the extrinsic CD bands. This was indeed observed by lowering the pH from 7.56 to 4.35; according to the CD–pH titration curve displayed in **Figure 6**, only 14% of piperine molecules are in a protein-bound state at pH 4.35, whereas the transition midpoint is at pH 6.7, at which 50% of the ligand molecules have already been released. The acidic blue shift of the UV band and the elevation of the absorption baseline (inset in **Figure 6**) are both indicative of

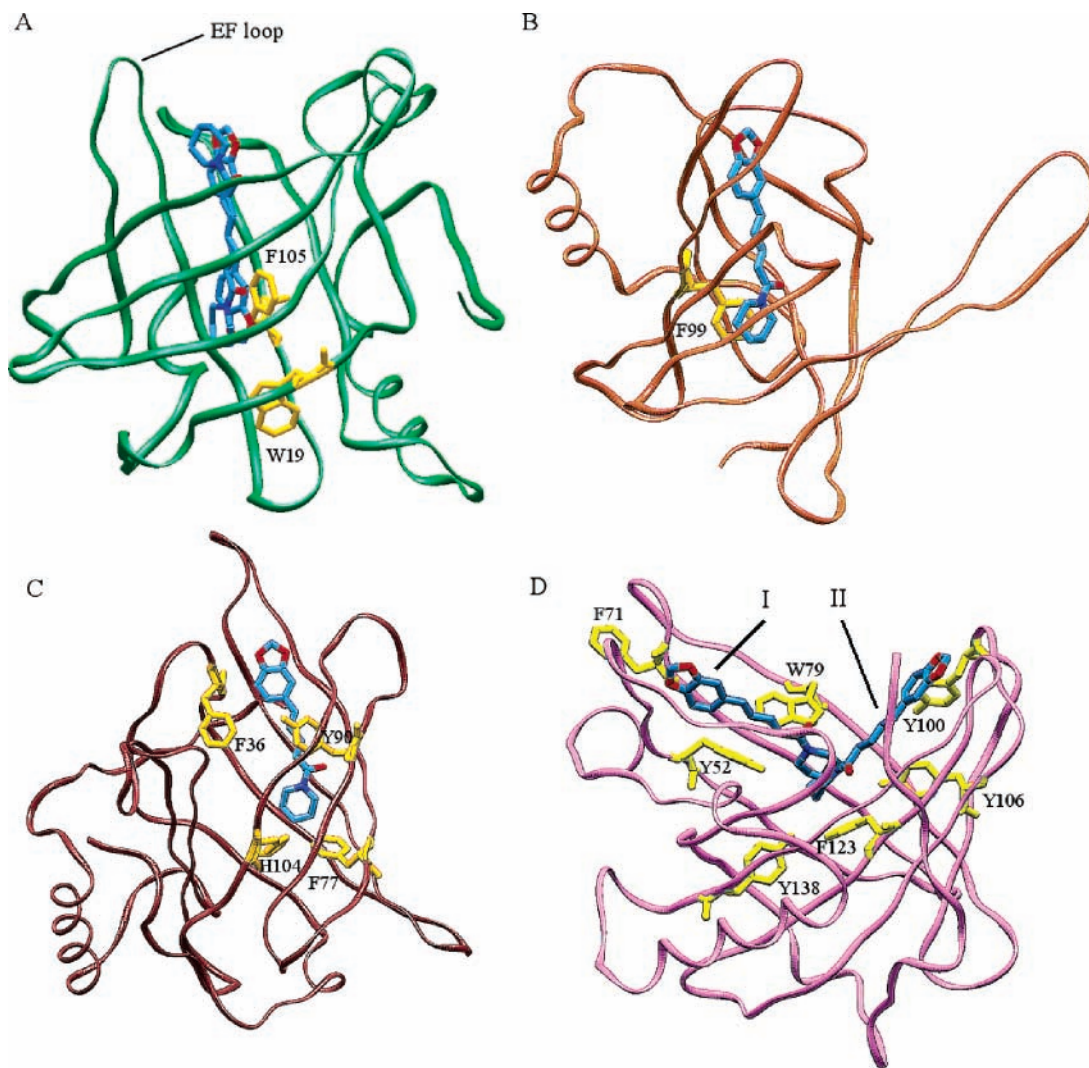


**Figure 8.** Molecular models of lipocalin proteins complexed with piperine: (A) Bovine  $\beta$ -lactoglobulin A; (B) human tear lipocalin; (C) human serum retinol binding protein; (D) human neutrophil gelatinase associated lipocalin. Only the best energy results obtained by docking calculations are shown. Protein secondary structures are shown schematically as solid ribbon models; the ligand molecules are displayed in a capped cylinder representation and colored by atom type (C, blue; O, red). Aromatic side chains and histidine residues of the lipocalin binding sites are identified by their one-letter code and highlighted in yellow (cf. Table 1). The figures were prepared using the Biodesigner program (v. 0.75).

the aqueous self-association of the free, protein-unbound piperine molecules. Because the movement of the EF loop is reversible, the binding site becomes accessible again when the pH value is raised. Indeed, the extrinsic CD bands reappeared when the pH of the sample solution was raised from 4.35 to 7.44 (Figure 6). Thus, the above results suggest the binding of piperine into the central cavity of BLG. To obtain further experimental evidence on the binding site of piperine, small aliquots of concentrated palmitic acid solution were added to a sample solution containing piperine and BLG-A at a ligand-to-protein ratio of 0.71. Monitoring the induced CD spectrum of piperine during the titration showed a rapid extinction of the extrinsic CD activity (Figure 7), indicating the displacement of piperine from its protein binding site by the fatty acid molecules. At the end of the titration the UV peak of piperine was shifted to shorter wavelengths by 2 nm (342.5  $\rightarrow$  340.5 nm). As has been unambiguously demonstrated by X-ray crystallography, palmitic acid binds in the central hole of the BLG (13); thus, it can safely be concluded that the binding site of piperine is also here.

**Molecular Modeling Studies of Piperine–Lipocalin Interactions.** Docking calculations were performed to gain

structural insight into the piperine–BLG interaction. In full agreement with the spectroscopic results, the piperine molecule could be docked into the central cavity of the protein (Figure 8). The central pocket is suitably sized for accommodating a single piperine molecule, and this binding mode yielded the best docking energy results, whereas the outer surface of the protein was found to provide no appropriate binding environment for piperine. The docking calculations suggested that binding of the piperine molecule may occur in two, energetically equivalent, ways: either the piperidine ring is buried within the pocket or it is positioned at the open entrance of the cavity (Figure 8). There is no conformational adaptation of the ligand required for its fitting into the binding pocket; in both forms the piperine molecule is essentially planar and the piperidine ring adopts the most stable chair conformation. Within van der Waals contact ( $<4.0$  Å), the conjugated hydrocarbon chain and aromatic ring of the ligand are surrounded by hydrophobic residues (Leu, Ile, Val, and Met) that line the wall of the cavity (Table 1). Inside the binding pocket, only one aromatic residue, Phe105, is in a suitable spatial orientation to establish  $\pi$ – $\pi$  stacking interaction with the aromatic ring of the piperine molecule, although Trp19 is also close enough to the methoxy

**Table 1.** Properties of the Piperine Binding Sites of Lipocalin Proteins As Found by Docking Calculations (cf. **Figure 8**)

|   | bovine $\beta$ -lactoglobulin-A | human tear lipocalin                     | human neutrophil gelatinase associated lipocalin (I) | human neutrophil gelatinase associated lipocalin (II) | human serum retinol binding protein          |
|---|---------------------------------|--|--|---|--|
| PDB ID  | 1QG5                            | 1XKI                                     | 1DFV   | 1DFV  | 1JYD   |
| aromatic side chains and histidine residues at the binding site | Phe105<br>Trp19                 | Phe99                                    | Tyr52<br>Phe71<br>Trp79<br>Tyr106                    | Trp79<br>Tyr100<br>Tyr106<br>Phe123<br>Tyr138         | Phe36<br>Phe77<br>Tyr90<br>His104            |
| no. of van der Waals contacts                                   | 102                             | 143                                      | 63   | 63  | 117  |
|   |                                 | intermolecular hydrogen bonds            |  |   |  |
| piperine heteroatoms  |                                 |  | protein residues                                     |   |  |
| C=O ( <i>amide</i> )  |                                 |  | Lys134   | Tyr106<br>Lys134                                      | <i>Leu37</i><br><i>Val74</i><br><i>Gln98</i> |
| -(H)N- ( <i>amide</i> )   |                                 | <i>Arg111</i>                            | Trp79<br>Lys134                                      | Tyr106  |  |
| -O- ( <i>meta</i> )   |                                 | Ser101<br>Lys114                         |  | Ser127  | <i>Gln98</i>                                 |
| -O- ( <i>para</i> )   |                                 | Ser101<br><i>Arg111</i><br><i>Gly112</i> | <i>Lys50</i>   |   | <i>Gly75</i>                                 |

<sup>a</sup> Backbone residues involved in intermolecular H-bonding with piperine are given in italic type.

groups ( $\approx 6$  Å). No intermolecular H bonds were found between the heteroatoms of the ligand and the binding site residues (**Table 1**). Overall, this picture suggests that piperine is held predominantly by hydrophobic interactions inside the cavity.

Because the  $\beta$ -barrel containing a highly hydrophobic interior is a common structural element of the lipocalin protein family and because the above results point out the " $\beta$ -barrel affinity" of piperine, further modeling studies were performed to investigate the binding of piperine to some human lipocalin proteins. X-ray structures of tear lipocalin (TL), neutrophil gelatinase associated lipocalin (NGAL), and serum retinol binding protein (RBP) were used for these docking calculations. In each case, the best docking energy results were obtained when piperine was bound in the central cavity of the  $\beta$ -barrel (**Figure 8**). In NGAL, two energetically equivalent docking results were obtained. In contrast to tear lipocalin, ligand binding sites of both NGAL and RBP are especially rich in aromatic residues (**Table 1**), suggesting the possible role of aromatic  $\pi$ - $\pi$  stacking interactions in anchoring the piperine molecule in the central pocket. Additionally, several intermolecular H bonds contribute to the stabilization of the ligand in all lipocalins linking the amide/methoxy moieties of piperine with polar side chains and the backbone of the protein host (**Table 1**). Interestingly, the number of van der Waals contacts between the ligand and the protein site is considerably lower in NGAL relative to the other lipocalins, including BLG. Indeed, the two ligand orientations in NGAL were found in the solvent-exposed, open mouth of the central cavity, where they were only partly buried by the side chains (**Figure 8**). Taken collectively, these data indicate that piperine might be the potential ligand of the above human lipocalins.

It is interesting to note that as a salivary protein, tear lipocalin is also highly expressed in the von Ebner's glands of the human tongue (25, 26). Thus, it may be hypothesized that this protein is involved in the perception of the pepper taste by binding the lipophilic piperine and transporting it to (or possibly away from) the taste buds. Additionally, like BLG, tear lipocalin also shows pH-dependent ligand binding controlled by a pH-driven conformational movement of two flexible loops at its calyx entrance (27). TL shows 27% amino acid sequence identity with BLG (28).

**Conclusions.** Piperine, the main component of the ancient medicinal spice pepper, has been reported to show numerous phytochemical benefits, however its interaction with mammalian biopolymers is still unexplored. Non-covalent association of piperine with the lipocalin member bovine  $\beta$ -lactoglobulin was shown by measuring extrinsic CD bands induced by the interaction of the ligand chromophore with the encompassing asymmetric protein environment. Both the CD displacement experiment using palmitic acid and the pH-dependent reversible change of the induced CD spectrum indicated a single piperine molecule to be bound in the central hydrophobic cavity of BLG. The pH tunable binding of piperine makes BLG a potential carrier for this hydrophobic drug in biological fluids and provides an experimental basis to engineer novel BLG variants (site-directed mutagenesis) with higher piperine binding affinity. Computational docking calculations revealed that piperine also fits well in the  $\beta$ -barrel of human lipocalins involved in inflammatory processes and serum retinoid transport, although in these cases binding involves both H-bonding and hydrophobic forces. These results highlight the potential role of lipocalins in mediating the diverse pharmacological activities of this important dietary alkaloid.

#### ABBREVIATIONS USED

BLG, bovine  $\beta$ -lactoglobulin; CD, circular dichroism; CE, Cotton effect; L/P, ligand/protein molar ratio; mdeg, millidegree; NGAL, human neutrophil gelatinase associated lipocalin; RBP, human serum retinol binding protein; TL, human tear lipocalin; UV, ultraviolet.

#### ACKNOWLEDGMENT

We thank Dr. Zsolt Bikádi for his assistance in the molecular modeling calculations.

#### LITERATURE CITED

- Vijayakumar, R. S.; Surya, D.; Nalini, N. Antioxidant efficacy of black pepper (*Piper nigrum* L.) and piperine in rats with high fat diet induced oxidative stress. *Redox Rep.* **2004**, *9*, 105–110.

- (2) Mittal, R.; Gupta, R. L. In vitro antioxidant activity of piperine. *Methods Find. Exp. Clin. Pharmacol.* **2000**, *22*, 271–274.
- (3) Koul, S.; Koul, J. L.; Taneja, S. C.; Dhar, K. L.; Jamwal, D. S.; Singh, K.; Reen, R. K.; Singh, J. Structure–activity relationship of piperine and its synthetic analogues for their inhibitory potentials of rat hepatic microsomal constitutive and inducible cytochrome P450 activities. *Bioorg. Med. Chem.* **2000**, *8*, 251–268.
- (4) Kong, L. D.; Cheng, C. H.; Tan, R. X. Inhibition of MAO A and B by some plant-derived alkaloids, phenols and anthraquinones. *J. Ethnopharmacol.* **2004**, *91*, 351–355.
- (5) Sunila, E. S.; Kuttan, G. Immunomodulatory and antitumor activity of *Piper longum* Linn. and piperine. *J. Ethnopharmacol.* **2004**, *90*, 339–346.
- (6) Pradeep, C. R.; Kuttan, G. Effect of piperine on the inhibition of lung metastasis induced B16F-10 melanoma cells in mice. *Clin. Exp. Metastasis* **2002**, *19*, 703–708.
- (7) Pradeep, C. R.; Kuttan, G. Piperine is a potent inhibitor of nuclear factor-kappaB (NF-kappaB), c-Fos, CREB, ATF-2 and proinflammatory cytokine gene expression in B16F-10 melanoma cells. *Int. Immunopharmacol.* **2004**, *4*, 1795–1803.
- (8) Ribeiro, T. S.; Freire-de-Lima, L.; Previato, J. O.; Mendonca-Previato, L.; Heise, N.; de Lima, M. E. Toxic effects of natural piperine and its derivatives on epimastigotes and amastigotes of *Trypanosoma cruzi*. *Bioorg. Med. Chem. Lett.* **2004**, *14*, 3555–3558.
- (9) Flower, D. R.; North, A. C.; Sansom, C. E. The lipocalin protein family: structural and sequence overview. *Biochim. Biophys. Acta* **2000**, *1482*, 9–24.
- (10) Schlehuber, S.; Skerra, A. Lipocalins in drug discovery: from natural ligand-binding proteins to “anticalins”. *Drug Discov. Today* **2005**, *10*, 23–33.
- (11) Sawyer, L.; Kontopidis, G. The core lipocalin, bovine  $\beta$ -lactoglobulin. *Biochim. Biophys. Acta* **2000**, *1482*, 136–148.
- (12) Kontopidis, G.; Holt, C.; Sawyer, L. Invited review:  $\beta$ -lactoglobulin: binding properties, structure, and function. *J. Dairy Sci.* **2004**, *87*, 785–796.
- (13) Wu, S. Y.; Perez, M. D.; Puyol, P.; Sawyer, L.  $\beta$ -lactoglobulin binds palmitate within its central cavity. *J. Biol. Chem.* **1999**, *274*, 170–174.
- (14) Qin, B. Y.; Creamer, L. K.; Baker, E. N.; Jameson, G. B. 12-Bromododecanoic acid binds inside the calyx of bovine  $\beta$ -lactoglobulin. *FEBS Lett.* **1998**, *438*, 272–278.
- (15) Kontopidis, G.; Holt, C.; Sawyer, L. The ligand-binding site of bovine  $\beta$ -lactoglobulin: evidence for a function? *J. Mol. Biol.* **2002**, *318*, 1043–1055.
- (16) Dufour, E.; Roger, P.; Haertle, T. Binding of benzo[a]pyrene, ellipticine, and *cis*-parinaric acid to  $\beta$ -lactoglobulin: influence of protein modifications. *J. Protein Chem.* **1992**, *11*, 645–652.
- (17) Dufour, E.; Haertle, T. Binding of retinoids and  $\beta$ -carotene to  $\beta$ -lactoglobulin. Influence of protein modifications. *Biochim. Biophys. Acta* **1991**, *1079*, 316–320.
- (18) Chatterjee, A.; Dutta, C. P. Structure of piperlonguminine, an alkaloid of *Piper longum* Linn. *Tetrahedron Lett.* **1966**, *7*, 1797–1800.
- (19) Dufour, E.; Robert, P.; Bertrand, D.; Haertle, T. Conformation changes of  $\beta$ -lactoglobulin: an ATR infrared spectroscopic study of the effect of pH and ethanol. *J. Protein Chem.* **1994**, *13*, 143–149.
- (20) Zsila, F.; Bikádi, Z.; Simonyi, M. Induced chirality upon crocetin binding to human serum albumin: origin and nature. *Tetrahedron: Asymmetry* **2001**, *12*, 3125–3137.
- (21) Sreerama, N.; Woody, R. W. Computation and analysis of protein circular dichroism spectra. *Methods Enzymol.* **2004**, *383*, 318–351.
- (22) Fugate, R. D.; Song, P. S. Spectroscopic characterization of  $\beta$ -lactoglobulin–retinol complex. *Biochim. Biophys. Acta* **1980**, *625*, 28–42.
- (23) Qin, B. Y.; Bewley, M. C.; Creamer, L. K.; Baker, H. M.; Baker, E. N.; Jameson, G. B. Structural basis of the Tanford transition of bovine  $\beta$ -lactoglobulin. *Biochemistry* **1998**, *37*, 14014–14023.
- (24) Ragona, L.; Fogolari, F.; Catalano, M.; Ugolini, R.; Zetta, L.; Molinari, H. EF loop conformational change triggers ligand binding in  $\beta$ -lactoglobulins. *J. Biol. Chem.* **2003**, *278*, 38840–38846.
- (25) Redl, B. Human tear lipocalin. *Biochim. Biophys. Acta* **2000**, *1482*, 241–248.
- (26) Breustedt, D. A.; Korndorfer, I. P.; Redl, B.; Skerra, A. The 1.8 Å crystal structure of human tear lipocalin reveals an extended branched cavity with capacity for multiple ligands. *J. Biol. Chem.* **2005**, *280*, 484–493.
- (27) Gasymov, O. K.; Abduragimov, A. R.; Yusifov, T. N.; Glasgow, B. J. Interstrand loops CD and EF act as pH-dependent gates to regulate fatty acid ligand binding in tear lipocalin. *Biochemistry* **2004**, *43*, 12894–12904.
- (28) Redl, B.; Holzfeind, P.; Lottspeich, F. cDNA cloning and sequencing reveals human tear prealbumin to be a member of the lipophilic-ligand carrier protein superfamily. *J. Biol. Chem.* **1992**, *267*, 20282–20287.

---

Received for review August 9, 2005. Revised manuscript received September 30, 2005. Accepted October 25, 2005. This study was supported by Grant 1/A/005/2004 NKFP MediChem 2.

JF051944G